catalysts

MDPI

Article

Organically Functionalized Porous Aluminum Phosphonate for Efficient Synthesis of 5-Hydroxymethylfurfural from Carbohydrates

Riddhi Mitra, Bhabani Malakar and Asim Bhaumik *

School of Materials Sciences, Indian Association for the Cultivation of Science, 2A & 2B Raja S. C. Mullick Road, Jadavpur, Kolkata 700032, India; smsrm2633@iacs.res.in (R.M.); scsbm2857@iacs.res.in (B.M.)
* Correspondence: msab@iacs.res.in

Abstract: Naturally occurring fossil fuels are the major resource of energy in our everyday life, but with the huge technological development over the years and subsequent energy demand, the reserve of this energy resource is depleting at an alarming rate, which will challenge our net energy resources in the near future. Thus, an alternative sustainable energy resource involving biomass and bio-refinery has become the most emerging and demanding approach, where biofuels can be derived effectively from abundant biomass via valuable chemical intermediates like 5-hydroxymethylfurfural (5-HMF). 5-HMF is a valuable platform chemical for the synthesis of fuel and fine chemicals. Herein, we report the synthesis of the organically functionalized porous aluminum phosphonate materials: Ph-ALPO-1 in the absence of any template and Ph-ALPO-2 by using 1,3-diaminopropane-N,N,N′,N′-tetraacetic acid as a small organic molecule template and phenylphosphonic acid as a phosphate source. These hybrid phosphonates are used as acid catalysts for the synthesis of 5-HMF from carbohydrates derived from biomass resources. These Ph-ALPO-1 and Ph-ALPO-2 materials catalyzed the dehydration of fructose to 5-HMF with total yields of 74.6% and 90.7%, respectively, in the presence of microwave-assisted optimized reaction conditions.

Keywords: aluminum phosphate ($AlPO_4$); microporous and mesoporous materials; biomass conversion; 5-hydroxymethylfurfural (5-HMF); organic–inorganic hybrids

Citation: Mitra, R.; Malakar, B.; Bhaumik, A. Organically Functionalized Porous Aluminum Phosphonate for Efficient Synthesis of 5-Hydroxymethylfurfural from Carbohydrates. *Catalysts* **2023**, *13*, 1449. https://doi.org/10.3390/catal13111449

Academic Editors: José María Encinar Martín and Sergio Nogales Delgado

Received: 16 October 2023
Revised: 13 November 2023
Accepted: 16 November 2023
Published: 19 November 2023

1. Introduction

With the continuous depletion of fossil fuels as result of industrialization the global attention seeks to identify alternative renewable energy sources to overcome a future worldwide energy crisis [1–3]. Thus, the concept of "biomass valorization" has emerged as a pivotal solution at the intersection of science, technology, and sustainability [4–6]. Biomass is described as the renewable organics that can come from flora and fauna. Hence, biomass is the largest feedstock for alternative renewable energy resources available in nature. The majority of biomass resources consist of carbohydrates, bearing hexose (C6) and pentose (C_5)-based sugars [7]. Thus, carbohydrates derived from plants, agricultural waste, and forestry residues have gained considerable attention as a renewable and sustainable energy feedstock. These biomass-derived organic molecules can be converted into biofuels through various chemical and biochemical processes, offering an alternative to fossil fuels. The synthesis of biofuels from biomass involves transformation of the complex organic molecules present in biomass into simpler hydrocarbon compounds that can be used as 'fine platform chemicals' [8]. This process utilizes different technologies and pathways, each one having its own advantages and challenges.

Hence, carbohydrates have widespread potential to produce essential chemicals, which can otherwise be derived directly from petroleum resources. 5-HMF, consisting of a furan ring along with aldehyde and primary alcohol functional groups, is considered as one of the most essential biomass-derived platform chemicals by the US Department of

Energy [9]. This makes 5-HMF an effective intermediate, which can further be converted to many valuable products like 2,5-dimethylfuran, an essential biofuel [10,11]. That is why 5-HMF is also known as 'sleeping giant' in the field of intermediate chemistry [12]. Monosaccharides like fructose, glucose, etc., in the presence of acid catalysts, easily dehydrate to yield 5-HMF [13]. According to the literature to date, several mineral acids already showed high catalytic activity towards the synthesis of 5-HMF from different carbohydrates [14]. However, there are many obstacles of using these homogeneous catalysts, like separation from reaction mixture, recyclability, etc. Thus, heterogeneous catalysts have become an emerging choice for researchers in catalyzing these reactions [15–17]. Although many heterogeneous solid acid catalysts are reported in the literature for the 5-HMF synthesis from carbohydrate resources, organically functionalized porous materials can be the superior contenders over others due to their high specific surface area and inherent surface hydrophobicity for the guest molecules to react at the catalytic site [18–20]. Further, monodispersity in the particle size and Lewis acidity of the framework metals may improve catalytic performance of solid acid catalysis.

Crystalline microporous and mesoporous materials are intensively studied over the past half-century due to their high specific surface area, high thermal and chemical stability, and wide diversity in the framework architectures [21–23]. Among them phosphonate-based porous frameworks are of particular interest due to the chemistry involved between the trivalent metal cation (MO_4) tetrahedra and phosphate tetrahedral sites [24,25]. Open frameworks and high surface area (internal surface) could strengthen their catalytic and adsorption abilities. The construction of organic–inorganic hybrid porous materials is a rapidly expanding field of materials chemistry for the synthesis of the materials having specific structural entity and functionality [26]. Metal phosphonates, having organic functionality in the framework, is one such group of hybrid materials, which attracted extensive interest due to their emerging applications in many areas like ion-exchange, catalysis, charge storage, sensing, etc. [27]. Metal phenyl phosphonates represent a particularly important class of organic–inorganic hybrid materials having covalent bonds between the inorganic cluster and organic phenyl moieties [28]. To date, a large number of microporous $AlPO_4$ frameworks have been synthesized via a soft-templating route, containing 8–18 ring pore apertures (Figure 1), where small organic molecules like primary/secondary/tertiary amines and quaternary ammonium salts act as a template in directing the crystal structure and inbuilt nanoscale porosities [29].

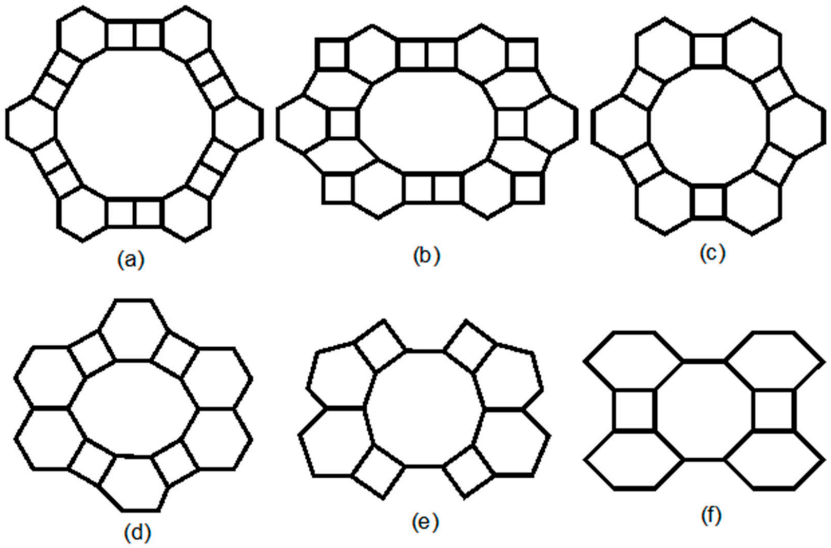

Figure 1. Different reported $AlPO_4$-n frameworks with various nanoscale pore openings (**a**) VPI-5 (18-ring), (**b**) $ALPO_4$-8 (14-ring), (**c**) $ALPO_4$-5 (12-ring), (**d**) $ALPO_4$-11 (10-ring), (**e**) $ALPO_4$-41 (10-ring), (**f**) $ALPO_4$-25 (8-ring).

In this context, it is pertinent to mention that the catalysis under microwave irradiation conditions is considered as a green chemical approach for the synthesis of small organic molecules. Microwave irradiation heats up the entire reaction mixture from its core through the polarization of the medium. So, generally polar solvents like DMSO, DMF, acetonitrile, etc., are used as medium of the microwave-assisted reactions. Further, aging and decomposition of 5-HMF in prolonged storing is a major issue [30], which could be considerably decreased if we could develop strategies for synthesizing 5-HMF from carbohydrates having no impurity of humins in the product.

In this work, we have synthesized phenyl functionalized organic–inorganic hybrid porous aluminum phosphonate materials Ph-ALPO-1 and Ph-ALPO-2, respectively, in the absence and presence of an organic additive 1,3-diaminopropane-N,N,N′,N′-tetraacetic acid in the synthesis mixture. These hybrid materials have then been used as heterogeneous catalyst for 5-HMF synthesis from carbohydrates under microwave-assisted heating conditions.

2. Results

The wide-angle powder X-ray diffraction (PXRD) of both Ph-ALPO-1 and Ph-ALPO-2 materials was studied for understanding the crystalline phase of these materials. Both samples exhibited sharp peak at 2θ = 5.08°. PXRD data collected in the range of 4° to 40° 2θ has been analyzed using the Expo2014 software package [31]. Ph-ALPO-1/2 materials are identified as lamellar structure with triclinic phase, P1 symmetry and the unit cell parameters are a =17.61 Å, b = 6.79 Å, and c = 4.88 Å, α = 106.690°, β = 94.204°, and γ = 80.948°. The diffraction peaks are indexed in Table S1 (Supporting Information). The resemblance of PXRD patterns for both Ph-ALPO-1 and Ph-ALPO-2 indicates the structure remains unchanged by using the template molecule in the synthesis (Figure 2A). However, a considerable improvement in the crystallinity was observed for Ph-ALPO-2; the sample was synthesized in the presence of the template. In order to measure the permanent porosity and the surface area of both the materials, we have analyzed N_2 adsorption–desorption analysis at 77 K. A high nitrogen uptake at low P/P_0 followed by slow and steady capillary condensation at higher P/P_0 indicates a mixture of type-I and type-IV isotherms has been observed (Figure 2B) [32]. Consequently, the pore size distribution (PSD) plots were calculated from these isotherms using NLDFT model (Figure 2C). These PSD plots suggested a hierarchical porosity with a peak micropore at 1.3 nm. Whereas Ph-ALPO-2 displayed a distinct mesopore at 5.8 nm, the peak for mesopores of Ph-ALPO-1 remains much distributed suggesting template plays a crucial role in organizing the overall framework rigid, organized and porous. Again, the pore volume of Ph-ALPO-1 and Ph-ALPO-2 comes out as 0.38 cc g^{-1} and 0.63 cc g^{-1}, respectively. Ph-ALPO-1 and Ph-ALPO-2 showed the Brunauer–Emmett–Teller (BET) specific surface areas of 73 and 106 m^2g^{-1}, respectively. Larger BET surface area of Ph-ALPO-2 over Ph-ALPO-1 again suggests the advantage of using organic template in the synthesis of this porous aluminum phosphonate framework. A greater surface area is always beneficial for the application in catalysis or sorption application. Fourier-transformed infrared spectra of both the materials were investigated for understanding the bonding connectivity of both the materials. Both of the samples displayed almost similar spectral features (Figure 2D). In the spectra, wavenumber of 4000 to 400 cm^{-1} was selected for detailed study of the bonding connectivity of the materials. An overlaying between the bands of the vibrational bending of H-O-H of the hydration water at ~1620 cm^{-1} and the sharp stretching band of the phenyl group (ν_{C-C}) at ~1595 cm^{-1} has been observed. The band at 3000 cm^{-1} could be attributed to the C-H vibrational stretching and the band at ~1490 and ~1440 cm^{-1} indicate the skeletal vibrations of the rings. The intense and broad band in between ~3600 and ~3200 cm^{-1} is attributed to the O-H vibrational stretching due to the presence of hydration water. Another two bands in this region have been observed, i.e., one very sharp at ~3640 cm^{-1} is probably indicating the presence of adsorbed water having no interaction by H-bonding and the other broader near ~3510 cm^{-1} is clearly indicating this water molecule interacting weakly

through H-bonds [33]. The other stretching and bending modes of the Al-O-P bonds are shown in Figure 2D.

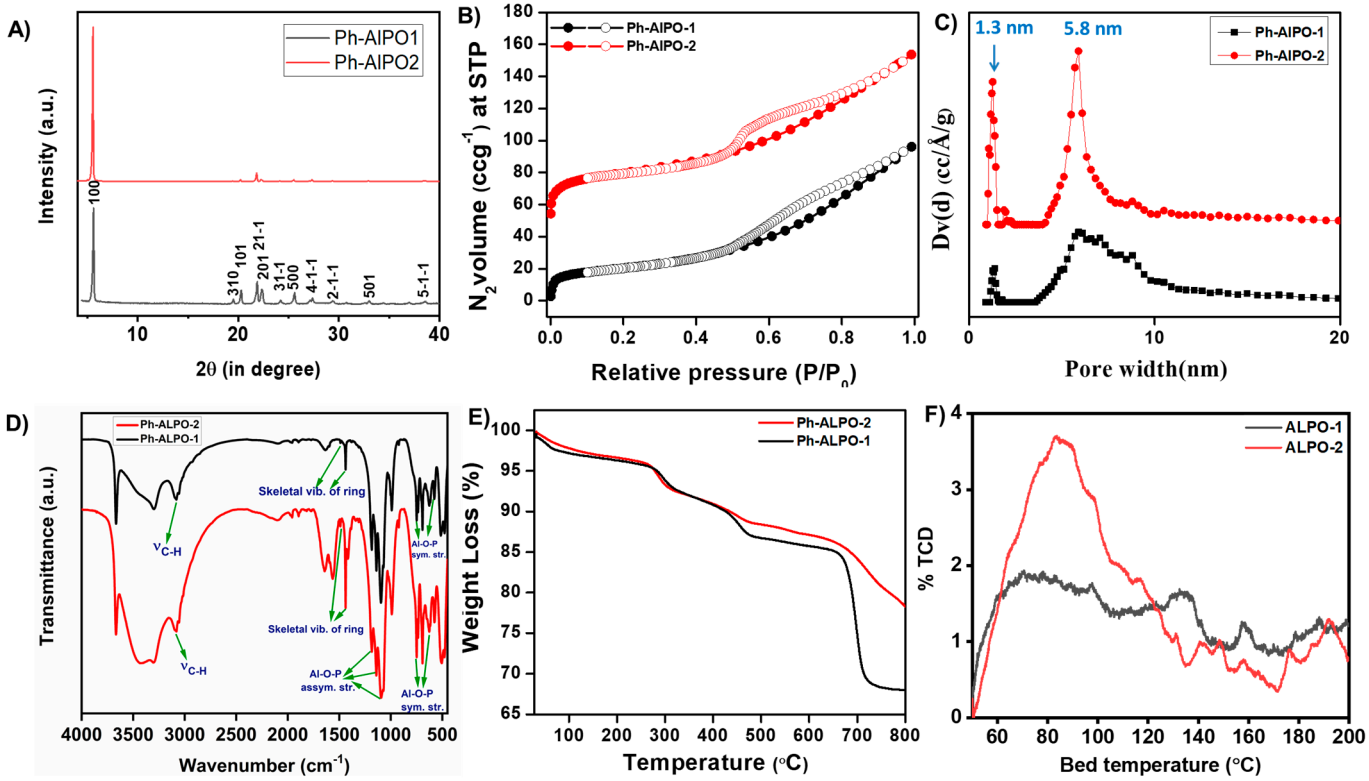

Figure 2. (**A**) Powder XRD patterns of Ph-ALPO-1 (black) and Ph-ALPO-2 (red), (**B**) N_2 adsorption/desorption isotherm of Ph-ALPO-1 (black) and Ph-ALPO-2 (red), (**C**) Non-local density functional theory (NLDFT) pore size distribution (PSD) of Ph-ALPO-1 (black) and Ph-ALPO-2 (red), (**D**) FT-IR spectra of Ph-ALPO-1 (black) and Ph-ALPO-2 (red), (**E**) Thermogravimetric curve of Ph-ALPO-1 (black) and Ph-ALPO-2 (red), (**F**) NH_3-TPD curve of Ph-ALPO-1 (black) and Ph-ALPO-2 (red).

Thermal stability of Ph-ALPO-1 and Ph-ALPO-2 materials was investigated through thermogravimetric analysis (TGA). The TGA analysis data was plotted in Figure 2E. Both the samples showed triplicate degradation between 25 and 800 °C. The first two mass losses between 6 and 15% occurred below 220 °C that are associated with an endothermic peak, which is because of desorption of physiosorbed and chemisorbed water molecules in the pores of the materials. The next mass loss occurs at temperatures higher than 250 °C, which is mainly due to the different degradation processes of organic matter. The mass loss recorded in this temperature range is about 8–10%. In the comparative TGA curves of both the materials, it clearly indicates that the final mass loss of Ph-ALPO-1 occurs at a faster rate than Ph-ALPO-2, which in turn clearly suggested the stability of the AlPO framework synthesized in the presence of the template molecule. Temperature-programmed desorption of ammonia (NH_3-TPD) analysis of both the materials was carried out under an inert He gas flow, and the corresponding 10% NH_3/He gas mixture desorption profile of ALPO-1 and ALPO-2 is shown in Figure 2F. From the NH_3-TPD profiles, it is seen that a broad NH_3 desorption peak centered around 80 °C was observed for both Ph-ALPO-1 and Ph-ALPO-2. This result suggested that NH_3 molecules are weekly bound in ALPO-1 and 2 surfaces. The observed total acidity of Ph-ALPO-1 and Ph-ALPO-2 were 92.59 and 285.82 $\mu molg^{-1}$, respectively. Considerably higher acidity of Ph-ALPO-2 synthesized in the presence of the template has motivated us to explore its catalytic activity.

The morphology of both the hybrid AlPO materials has been investigated by transmission electron microscopic analysis (FEG-TEM). All the electron microscopic images are

shown in Figure 3A–D. From the images, it was clearly shown that Ph-ALPO-1 shows irregular morphology (Figure 3A,B). Several 20–30 nm rod like particles are clearly visible for Ph-ALPO-1. However, these particles are irregularly nucleating to form several other morphologies as well (Figure 3A,B). But, one of our major objectives was to control the morphology of these nanoparticles, which could help in the catalytic reaction. We found that the small molecular template modification for the synthesis of Ph-ALPO-2 not only organize the particle morphology but also it hinders the agglomeration to generate monodisperse rod like nanoparticles of average size 20–30 nm (Figure 3C,D). The elemental mapping images shown in Figure 3E–H also confirms the template removal in Ph-ALPO-2 framework as no traces of "N" (comes from the template molecule) was found in the overall specimen. It is pertinent to mention that uniform distribution of C, O, P, and Al percentages in Ph-ALPO-2 (Figure 3E–H) also suggested the advantage of the phenyl functionalization of the AlPO framework via our above-mentioned process.

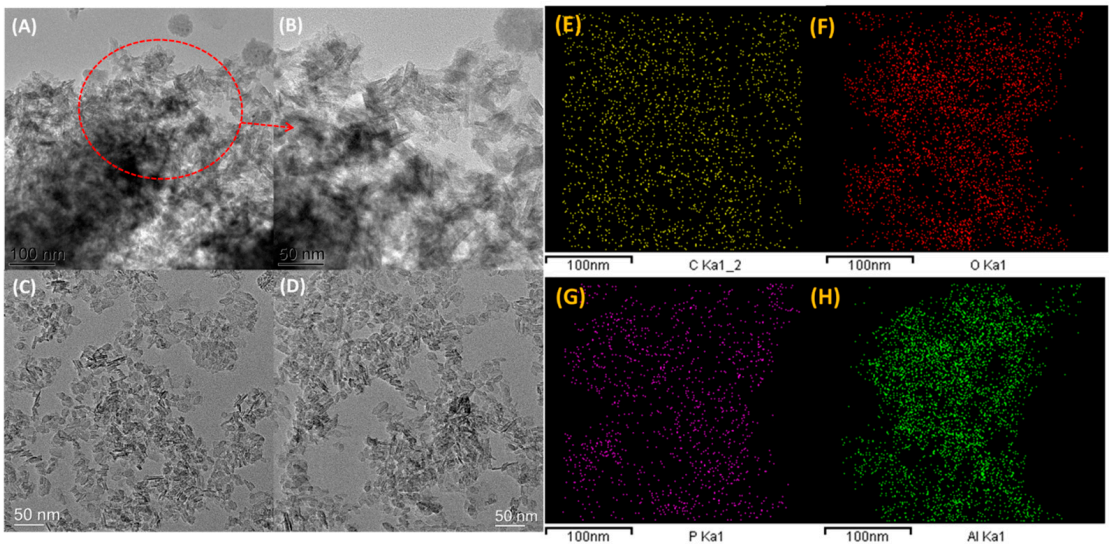

Figure 3. UHR-TEM images of Ph-ALPO-1 (**A**,**B**) and Ph-ALPO-2 (**C**,**D**). (**E**–**H**) are the C, O, P and Al elemental mapping data in Ph-ALPO-2.

3. Discussion

3.1. Catalytic Properties

3.1.1. Catalysis with Ph-ALPO-2

The 5-HMF synthesis from carbohydrates involve an acid catalyzed dehydration reaction and this has been extensively studied over the years. From the above characterizations and discussion of results, Ph-ALPO-2 could be a more promising material for acid catalysis compared to Ph-ALPO-1 as although both the materials have similar bonding connectivity and framework, Ph-ALPO-2 has more surface area than Ph-ALPO-1. Different carbohydrate precursors can be employed for the synthesis of 5-HMF by varying the monosaccharides. For optimizing the reaction conditions with maximum 5-HMF yield we have varied four major factors like the amount of catalyst loading, reaction temperature, reaction time, and choice of medium.

At first, taking fructose as the substrate and keeping all other parameters constant, we have performed the reaction by varying the catalyst amount from 7.08 wt % to 31.4 wt % to optimize the amount of catalyst needed for maximum 5-HMF yield. Figure 4A shows the different 5-HMF yield as a function of amount of given catalyst for fructose as the substrate. We have observed that upon increasing the catalyst amount from 2 mg up to 6 mg, the yield of the product has increased but further increases in the catalyst amount from 6 mg to 8 mg results in decreasing the product yield. From Figure 4A the relatively highest yield becomes 68.45% which was found for 6 mg of catalyst.

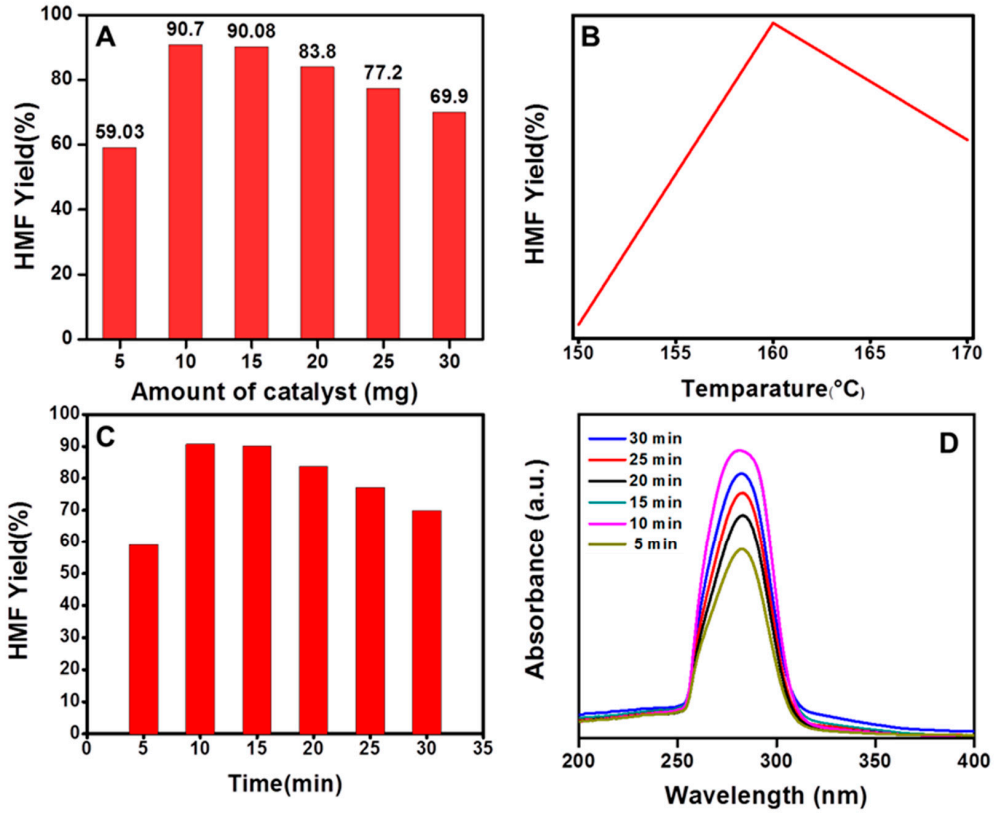

Figure 4. (**A**) Dependence of 5-HMF yield (%) on amount of catalyst; (**B**) Temperature dependence of 5-HMF yield (%); (**C**) Time dependence of 5-HMF yield (%) at the reaction temperature of 160 °C; (**D**) UV-Visible spectra of the product 5-HMF with reaction time (5–30 min). Typical standard deviation in the 5-HMF yield is ±1%.

Now we have carried out the reaction by varying the temperature from 140 °C to 170 °C with the similar carbohydrate substrate to observe the temperature dependence of the reaction on the product yield and the yield vs. temperature profile has been drawn from the 5-HMF yield (%) estimated through the UV-Visible spectrophotometric (shown in Figure 4B) studies. From this profile, the optimum temperature was 160 °C. At this temperature, fructose showed the highest yield for the 5-HMF in the presence of 6 mg of the catalyst for 15 min reaction time.

Then, we have plotted the 5-HMF yield as a function of reaction time from 5 min to 30 min at optimized temperature and catalyst amount by taking fructose as the substrate and we have drawn a suitable kinetic profile by calculating 5-HMF yield (%) through UV-Visible spectra using Beer–Lambert's law (Figure 4C). At 160 °C, 25.5 mg fructose shows the highest yield for the 5-HMF conversion reaction after 15 min reaction time with 6 mg aluminum phosphonate catalyst.

All these catalytic results are further tabularized in Table 1. Some observations seen from this table are, for example, that upon increasing the catalyst amount from 2 mg to 4 mg to 6 mg, the yield of the product has increased accordingly, but a further increase in the amount from 6 mg to 8 mg results in decreases in the product yield. The reason behind this observation may be that a certain increase in the catalyst gives a higher 5-HMF yield, as expected, according to an increasing number of acidic sites with the increasing amount of the catalyst, but a further increase in this catalyst amount after 6 mg reduces the product yield, which may be due to catalyst poisoning or further degradation of the main product by other byproducts. Again, a decreasing product yield was observed at further higher temperatures and longer reaction times. This may be attributed to the fact that a prolonged exposure time and higher reaction temperature may promote self- and cross-polymerization of 5-HMF with fructose, to yield the byproduct humins in the dehydration

step as the appearance of a dark-colored product in these cases has been observed in the reaction vial.

Table 1. Catalytic results of Ph-ALPO-2 for the 5-HMF formation under different conditions.

Sl. No.	Substrate Amount (mg)	Catalyst Amount (mg)	Temperature (°C)	Time (min.)	Yield (%)
1.	25.5	2	150	20	42.8
2.	25.5	4	150	20	56.04
3.	25.5	6	150	20	68.45
4.	25.5	8	150	20	63.92
5.	25.5	6	160	20	83.3
6.	25.5	6	170	20	76.09
7.	25.5	6	160	5	59.03
8.	25.5	6	160	10	90.08
9.	25.5	6	160	15	90.7
10.	25.5	6	160	25	77.2
11.	25.5	6	160	30	69.9

The formation of 5-HMF was confirmed from the 600 Hz ^{1}H NMR spectra of crude product mixture and the solution after solvent extraction using 'DCM-H_2O' mixture, and these are shown in Figure S1. The 150 Hz ^{13}C-NMR spectrum has also provided further confirmation of 5-HMF formation (Figure S2). The λ_{max} for 5-HMF in UV-Visible spectrum arises at ~284 cm^{-1} (Figure S3). From that characteristic peak using the Beer–Lambert's law the yield of 5-HMF (shown in Figure 4D) has been calculated. The maximum amount of 5-HMF, 90.7%, was found for 6 mg of Ph-ALPO-2 catalyst at 160 °C in 15 min, from 25.5 mg of fructose as the substrate.

Then, we have estimated the catalytic activity by varying the substrates using some common monosaccharides like glucose and galactose in the above optimized condition as shown in Figure 5B. We observed that glucose and galactose give an almost similar yield for 5-HMF, which is quite low compared to fructose itself. We have tried this reaction using different solvents like 'DMSO + H_2O', DMF, 'acetonitrile + H_2O', and NMP. The yields are calculated from the respective UV-Visible spectra and presented as a bar diagram in Figure 5A. Compared with DMSO, other solvents showed low yields of 5-HMF. This result suggested that in the case of DMSO, the maximum amount of energy is converted from microwave radiation, which transforms maximum fructose to 5-HMF. The decreasing trend of the 5-HMF yields was DMSO > DMSO + H_2O > NMP > DMF> acetonitrile + H_2O.

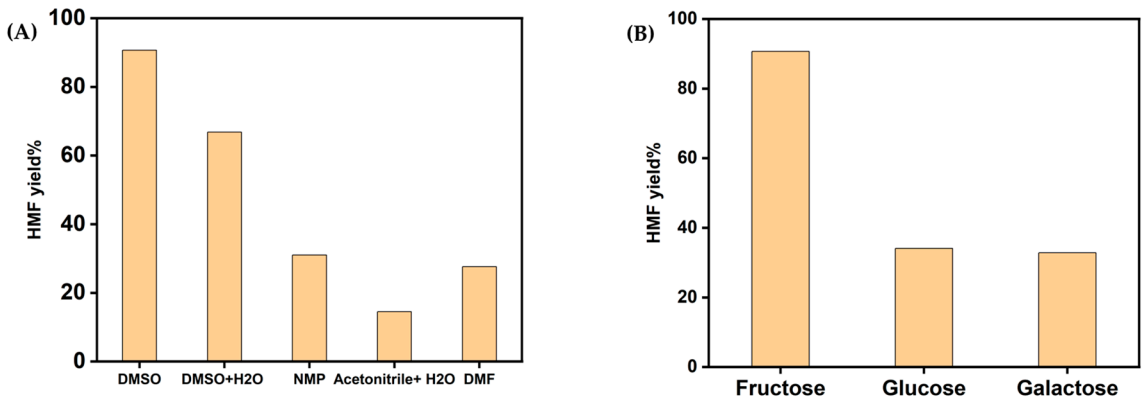

Figure 5. (**A**) Solvent dependence of substrate and (**B**) Selectivity of substrates for 5-HMF yield.

Further, we have performed the experiment with the lignocellulosic solid biomass (sugarcane pulp) also under optimized catalytic conditions. However, even after 30 min of microwave irradiation, we found a trace of 5-HMF only. This result suggested that Ph-ALPO-2 can catalyze the sugar content of the sugarcane pulp. Actually, when we use a solid biomass like lignin, after completion of the reaction, the lignin will form an insoluble physical mixture with the catalyst. As lignin has some solubility in DMSO, we tried to separate the catalyst through solvent extraction. But the wholesome biomass cannot be separated from the catalyst.

3.1.2. Catalysis with Ph-ALPO-1

With the above optimized condition, the 5-HMF yield from fructose in the case of Ph-ALPO-1 as the catalyst was 74.6% (as shown in Figure S4).

3.2. Role of Template in Synthesizing Phenyl Aluminophosphate Catalyst

From the nitrogen sorption isotherm, it is clear that Ph-ALPO-2, which has been synthesized using 1,3-diaminopropane-N,N,N′,N′-tetraacetic acid as a small-molecule template, has more surface area than Ph-ALPO-1, which has been synthesized in non-templated method. Again, from the TGA analysis, the framework of Ph-ALPO-2 shows higher stability than Ph-ALPO-1; i.e., upon using the template, the robustness of the framework of the AlPO material becomes much higher. Now, from the catalysis point of view, according to NH_3-TPD analysis, the template-based synthesized material shows higher active (acidic) sites than Ph-ALPO-1 (synthesized in non-templated method). As a result of all these above-mentioned facts, the yield of 5-HMF is also higher in the case of Ph-ALPO-2 in comparison with Ph-ALPO-1. These comparative results could be attributed to the fact that for generating porosity in the case of Ph-ALPO-2, the phenyl groups in phenylphosphonic acid is used as a spacer along with 1,3-diaminopropane-N,N,N′,N′-tetraacetic acid, which is used as a small-molecule template. But for Ph-ALPO-1, the pores are generated only due to the presence of phenyl spacer present in the phenylphosphonic acid. Thus, the higher BET surface area, crystallinity, and uniform particle morphology of the Ph-ALPO-2 catalyst synthesized in the presence of organic template are responsible for the higher yield of 5-HMF in this dehydration reaction.

3.3. Comparision of Ph-ALPO-2 with Other Catalysts in the Literature

The reaction parameters and corresponding yields of 5-HMF of this Ph-ALPO-2 material compared with those of related porous catalysts [34–38] available in the literature are tabularized in Table 2. From the results shown here, we can conclude that Ph-ALPO-2 displayed a considerably good catalytic efficiency for the synthesis of 5-HMF from biomass-derived fructose.

Table 2. Comparative study of catalytic efficiency in HMF conversion reaction between Ph-ALPO-1/2 and other zeo-type catalysts in the literature.

Catalyst	Temp. (°C)	Solvent	Time (min.)	Substrate	Yield (%)	Ref.
Al-KCC-1	162	DMSO	60	Fructose	92.9	[33]
NBPW-01	80	DMSO	180	Fructose	89	[34]
NBPW-06	80	DMSO	90	Fructose	96.7	[35]
Al-MCM-41	170	H_2O/MIBK	75	Fructose	42.3	[36]
LPSnP-1	120	H_2O/MIBK: 2-butanol	20	Fructose	77	[36]
TESAS-SBA-15	130	H_2O/MIBK: 2-butanol	141	Fructose	71	[37]
PHMS-2	160	DMSO	25	Fructose	83.7	[38]
Ph-ALPO-1	160	DMSO	15	Fructose	74.6	This work
Ph-ALPO-2	160	DMSO	15	Fructose	90.7	This work

4. Materials and Methods

4.1. Chemicals

Aluminum iso-propoxide, phenylphosphonic acid, liquid ammonia (25% aqueous), 1,3-diaminopropane-N,N,N′,N′-tetraacetic acid and fructose were purchased from Sigma Aldrich, Bangalore, India. All solvents were used after purification. Deionized water was used for synthesis and cleaning purposes.

4.2. Instrumentation

Powder X-ray diffraction data of aluminum phosphonates Ph-ALPO-1 and Ph-ALPO-2 were collected from a Bruker D-8 Advanced SWAX, Germany diffractometer using Ni-filtered Cu Kα (λ = 0.15406 nm) radiation. Specific surface area and porosity were analyzed from the N_2 sorption analysis at 77 K by using an Anton Paar Quanta Tec (USA) Isorb-HP-1 100 gas sorption analyzer. The pore-size distribution plots for both the materials were obtained from the non-local density functional theory (NLDFT) model. Both samples were dried and degassed at 150 °C for 5 h under high vacuum before the sorption analysis. Ultrahigh-resolution transmission electron microscopic (UHR-FEG TEM) system of JEOL JEM 2100F (Japan) working with at a 200 kV electron source, the particle size and nanostructure of the Ph-ALPO-1 and Ph-ALPO-2 frameworks were analyzed. Samples for these TEM analysis was prepared by dropping isopropanol solutions of both the materials into two separate carbon-coated copper grids and then drying them under a high vacuum. Using KBr pellets and by using a Shimadzu FT-IR 8400S (Japan) instrument, Fourier transform infrared (FT-IR) spectra of the samples were obtained. The Anton Paar Microwave Synthesis Reactor (Monowave 300, USA) was used for all of the catalysis experiments. For measuring the surface acidity of these aluminum phosphonate materials temperature-programmed desorption of ammonia (TPD-NH_3) analysis was carried out in an AMI-300 Lite Chemisorption Analyzer of Altramira Instruments LLC, USA.

4.3. Synthesis of Ph-ALPO-1

In a typical synthesis of Ph-ALPO-1, 204 mg (0.001 M) phenylphosphonic acid was dissolved in 18 mL deionized water and stirred for 30 min on a magnetic stirrer. Then, 158 mg (0.001 M) aluminum iso-propoxide was added in it and again stirred for another 15 min. After that liquid ammonia was added in dropwise manner until the pH of the solution becomes ~8.0. Then, it was again stirred for ~3 h. Then, the reaction mixture was transferred into a 30 mL Teflon-lined stainless-steel autoclave and placed in an oven at 170 °C for 3 days. After 3 days, aluminum phenylphosphonate material was formed. It was then separated and washed with water and methanol by centrifugation. The yield of the product becomes ~90 mg. Then, the product was collected in the Eppendorf and characterized thoroughly.

4.4. Synthesis of Ph-ALPO-2

In this stage, 306 mg (0.001M) 1,3-diaminopropane-N,N,N′,N′-tetraacetic acid was dissolved in 21 mL deionized water and stirred for 45 min. Then, 158 mg (0.001 M) phenylphosphonic acid was mixed in it and again stirred for another 30 min. Then, 204 mg (0.001 M) aluminum iso-propoxide was added in it and stirred for another 3 h. After that, liquid ammonia was added in a dropwise manner until the pH of the solution became ~8.0. Aluminum phenylphosphonate gel had been prepared. Now, this gel was transferred into a 30 mL Teflon-lined stainless-steel autoclave and placed in an oven at 170 °C for 3 days. After 3 days, an aluminum phenylphosphonate framework containing the template molecules was formed. It was then separated and washed with water and methanol by centrifugation. The yield of the product was ~120 mg.

4.5. Extraction of Template from Ph-ALPO-2

The as-synthesized product was taken in a beaker and stirred with 50% EtOH and 50% water for 6 h continuous stirring at room temperature. The extracted product was

then separated and washed with water and EtOH via centrifugation, and the product was collected in the Eppendorf and used for further application.

4.6. Activation of Catalyst

In order to remove adsorbed solvent molecules, which may partially impede catalytic activity by blocking some active sites, the catalysts are activated prior to the catalytic reaction. We activated all the catalysts (Ph-ALPO-1 and Ph-ALPO-2) at 120 °C for 6 h in a hot air oven before putting them into the catalysis chamber. For all subsequent catalytic experiments, a similar activation route for the catalysts was followed.

4.7. 5-HMF Synthesis

Here, fructose, glucose, and galactose were used as carbohydrate sources for the synthesis of 5-HMF. In a typical synthesis, the carbohydrate was charged with activated catalyst and DMSO (2 mL) in a microwave-safe G-10 vial. The vial was then correctly sealed and kept at the desired temperature for the above-mentioned amount of time in a microwave reactor. The internal pressure of the vial was initially nil. However, after the steady-state condition, the internal pressure was elevated to 5 bar. The temperature of the microwave was controlled by a previously set program; briefly, the final temperature was set as 160 °C for a holding time of 15 min with a continuous stirring speed of 600 rpm, and the reaction mixture was cooled to 25 °C to obtain the product. At 160 °C, the temperature at which the catalysis was optimized, 24% of the catalyst, Ph-ALPO-2, produced 90.7% HMF yield in DMSO medium in 15 min reaction time. Water and DCM were used to extract 5-HMF from the reaction mixture. In DMSO-d6 medium, the extracted product was examined via ^{1}H-NMR and ^{13}C-NMR spectroscopic analysis (distinctive signals of 5-HMF shown in Figures S1 and S2). Then, 5-HMF yield was calculated from the solution using UV-Visible spectrophotometry.

5. Conclusions

In this work, we have demonstrated the synthesis of a new porous organic–inorganic hybrid aluminum phosphonate framework material having a hydrophobic phenyl moiety at the pore surface in the presence and absence of a small organic molecule 1,3-diaminopropane-N,N,N′,N′-tetraacetic acid as a template via a hydrothermal synthetic route. We have successfully shown the crucial role of porosity and surface area, and the use of organic template in the hydrothermal synthesis for the catalytic application. The synthetic protocol and the catalytic results described here are cost-effective and environmentally friendly. Furthermore, these porous phenylphosphonates show the potential to synthesize 5-HMF from carbohydrates in a very high yield in a short reaction time using a green chemical route. Thus, the easy and convenient synthesis method reported herein could offer a new opportunity for researchers and industries for the sustainable synthesis of biofuel intermediates over organically functionalized aluminum phosphonates.

Supplementary Materials: The following supporting information can be downloaded at: https://www.mdpi.com/article/10.3390/catal13111449/s1, Indexing of powder XRD of Ph-AlPO-1/2 (Table S1), ^{1}H NMR (Figure S1) and ^{13}C-NMR (Figure S2) spectra of 5-HMF, UV-Visible characteristic peak of 5-HMF (Figure S3), and comparative catalytic activity of Ph-ALPO-1 and Ph-ALPO-2 through UV-Visible spectrophotometry (Figure S4).

Author Contributions: Experiments, investigation, and formal analysis were performed by R.M. B.M. involved in the formal analysis of the catalysts. A.B. provided the resources and conducted the investigation and overall supervision of this project. R.M. wrote the draft manuscript with the help of A.B. All authors have read and agreed to the published version of the manuscript.

Funding: BM wants to thank UGC, New Delhi (NTA Ref. No.: 221610080374), for a Junior Research Fellowship.

Data Availability Statement: Data is contained within the article.

Acknowledgments: RM wants to thank Anirban Ghosh for helping with the catalytic experiments and draft manuscript preparation and for contributing to useful scientific discussions. AB would like to acknowledge DST-SERB, New Delhi, for a Core Research Grant (Project no. CRG/2022/002812).

Conflicts of Interest: The authors declare no conflict of interest.

References

1. Höök, M.; Tang, X. Depletion of fossil fuels and anthropogenic climate change—A review. *Energy Policy* **2013**, *52*, 797–809. [CrossRef]
2. Ragauskas, A.J.; Williams, C.K.; Davison, B.H.; Britovsek, G.; Cairney, J.; Eckert, C.A.; Frederick, W.J.J.; Hallett, J.P.; Leak, D.J.; Liotta, C.L.; et al. The path forward for biofuels and biomaterials. *Science* **2006**, *311*, 484–489. [CrossRef] [PubMed]
3. Cunha, J.T.; Romani, A.; Domingues, L. Whole Cell Biocatalysis of 5-Hydroxymethylfurfural for Sustainable Biorefineries. *Catalysts* **2022**, *12*, 202. [CrossRef]
4. Barta, K.; Ford, P.C. Catalytic Conversion of Nonfood Woody Biomass Solids to Organic Liquids. *Acc. Chem. Res.* **2014**, *47*, 1503–1512. [CrossRef]
5. Corma, A.; Iborra, S.; Velty, A. Chemical Routes for the Transformation of Biomass into Chemicals. *Chem. Rev.* **2007**, *107*, 2411–2502.
6. Liu, Y.Z.; Chen, W.S.; Xia, Q.Q.; Guo, B.T.; Wang, Q.W.; Liu, S.X.; Liu, Y.X.; Li, J.; Yu, H.P. Efficient Cleavage of Lignin-Carbohydrate Complexes and Ultrafast Extraction of Lignin Oligomers from Wood Biomass by Microwave-Assisted Treatment with Deep Eutectic Solvent. *ChemSusChem* **2017**, *10*, 1692–1700. [CrossRef]
7. Chheda, J.N.; Roman-Leshkov, Y.; Dumesic, J.A. Production of 5-Hydroxymethylfurfural and Furfural by Dehydration of Biomass-Derived Mono- and Poly-Saccharides. *Green Chem.* **2007**, *9*, 342–350. [CrossRef]
8. Osatiashtiani, A.; Lee, A.F.; Brown, D.R.; Melero, J.A.; Morales, G.; Wilson, K. Bifunctional SO_4/ZrO_2 Catalysts for 5-Hydroxymethylfufural (5-HMF) Production from Glucose. *Catal. Sci. Technol.* **2014**, *4*, 333–342. [CrossRef]
9. Bozell, J.J.; Petersen, G.R. Technology Development for the Production of Biobased Products from Biorefinery Carbohydrates—The US Department of Energy's "Top 10" Revisited. *Green Chem.* **2010**, *12*, 539–554. [CrossRef]
10. Solanki, B.S.; Rode, C.V. Selective Hydrogenation of 5-HMF to 2,5-DMF Over a Magnetically Recoverable Non-Noble Metal Catalyst. *Green Chem.* **2019**, *21*, 6390–6406.
11. Cortez-Elizalde, J.; Córdova-Pérez, G.E.; Silahua-Pavón, A.A.; Pérez-Vidal, H.; Cervantes-Uribe, A.; Cordero-García, A.; Arévalo-Pérez, J.C.; Becerril-Altamirano, N.L.; Castillo-Gallegos, N.C.; Lunagómez-Rocha, M.A.; et al. 2,5-Dimethylfuran Production by Catalytic Hydrogenation of 5-Hydroxymethylfurfural Using Ni Supported on Al_2O_3-TiO_2-ZrO_2 Prepared by Sol-Gel Method: The Effect of Hydrogen Donors. *Molecules* **2022**, *27*, 4187. [CrossRef] [PubMed]
12. Tong, X.L.; Ma, Y.; Li, Y.D. Biomass into Chemicals: Conversion of Sugars to Furan Derivatives by Catalytic Processes. *Appl. Catal. A Gen.* **2010**, *385*, 1–13. [CrossRef]
13. Tempelman, C.H.L.; Oozeerally, R.; Degirmenci, V. Heterogeneous Catalysts for the Conversion of Glucose into 5-Hydroxymethyl Furfural. *Catalysts* **2021**, *11*, 861. [CrossRef]
14. Bains, R.; Kumar, A.; Chauhan, A.S.; Das, P. Dimethyl carbonate solvent assisted efficient conversion of lignocel lulosic biomass to 5-hydroxymethylfurfural and furfural. *Renew. Energy* **2022**, *197*, 237–243. [CrossRef]
15. Mondal, S.; Mondal, J.; Bhaumik, A. Sulfonated Porous Polymeric Nanofibers as an Efficient Solid Acid Catalyst for the Production of 5-Hydroxymethylfurfural from Biomass. *ChemCatChem* **2015**, *7*, 3570–3578. [CrossRef]
16. Yin, Y.; Ma, C.H.; Li, W.; Luo, S.; Zhang, Z.S.; Liu, S.X. Insights into Shape Selectivity and Acidity Control in NiO-Loaded Mesoporous SBA-15 Nanoreactors for Catalytic Conversion of Cellulose to 5-Hydroxymethylfurfural. *ACS Sustain. Chem. Eng.* **2022**, *10*, 17081–17093. [CrossRef]
17. Zhang, Y.Z.; Zhao, B.W.; Das, S.; Degirmenci, V.; Walton, R.L. Tuning the Hydrophobicity and Lewis Acidity of UiO-66-NO_2 with Decanoic Acid as Modulator to Optimise Conversion of Glucose to 5-Hydroxymethylfurfural. *Catalysts* **2022**, *12*, 1502. [CrossRef]
18. Elhamifar, D.; Nasr-Esfahani, M.; Karimi, B.; Moshkelgosha, R.; Shábani, A. Ionic Liquid and Sulfonic Acid Based Bifunctional Periodic Mesoporous Organosilica (BPMO-IL-SO_3H) as a Highly Efficient and Reusable Nanocatalyst for the Biginelli Reaction. *ChemCatChem* **2014**, *6*, 2593–2599.
19. Herbst, A.; Janiak, C. MOF Catalysts in Biomass Upgrading Towards Value-Added Fine Chemicals. *CrystEngComm* **2017**, *19*, 4092–4117.
20. Chongdar, S.; Bhattacharjee, S.; Bhanja, P.; Bhaumik, A. Porous organic–inorganic hybrid materials for catalysis, energy and environmental applications. *Chem. Commun.* **2022**, *58*, 3429–3460.
21. Lewis, D.W.; Willock, D.J.; Catlow, C.R.A.; Thomas, J.M.; Hutchings, G.J. De Novo Design of Structure-Directing Agents for the Synthesis of Microporous Solids. *Nature* **1996**, *382*, 604–606. [CrossRef]
22. Cundy, C.S.; Cox, P.A. The Hydrothermal Synthesis of Zeolites: Precursors, Intermediates and Reaction Mechanism. *Microporous Mesoporous Mater.* **2005**, *82*, 1–78.
23. Jiang, J.X.; Yu, J.H.; Corma, A. Extra-Large-Pore Zeolites: Bridging the Gap between Micro and Mesoporous Structures. *Angew. Chem. Int. Ed.* **2010**, *49*, 3120–3145. [CrossRef] [PubMed]

24. Wilson, S.T.; Lok, B.M.; Messina, C.A.; Cannan, T.R.; Flanigen, E.M. Aluminophosphate Molecular Sieves: A New Class of Microporous Crystalline Inorganic Solids. *J. Am. Chem. Soc.* **1982**, *104*, 1146–1147. [CrossRef]
25. Davis, M.E.; Saldarriaga, C.; Montes, C.; Garces, J.; Crowder, C. A Molecular-Sieve With 18-Membered Rings. *Nature* **1988**, *331*, 698–699. [CrossRef]
26. Mizoshita, N.; Tani, T.; Inagaki, S. Syntheses, Properties and Applications of Periodic Mesoporous Organosilicas Prepared from Bridged Organosilane Precursors. *Chem. Soc. Rev.* **2011**, *40*, 789–800. [CrossRef]
27. Bhanja, P.; Na, J.; Jing, T.; Lin, J.J.; Wakihara, T.; Bhaumik, A.; Yamauchi, Y. Nanoarchitectured Metal Phosphates and Phosphonates: A New Material Horizon toward Emerging Applications. *Chem. Mater.* **2019**, *31*, 5343–5362. [CrossRef]
28. Gagnon, K.J.; Perry, H.P.; Clearfield, A. Conventional and Unconventional Metal-Organic Frameworks Based on Phosphonate Ligands: MOFs and UMOFs. *Chem. Rev.* **2012**, *112*, 1034–1054. [CrossRef]
29. Li, J.Y.; Qi, M.; Kong, J.; Wang, J.Z.; Yan, Y.; Huo, W.F.; Yu, J.H.; Xu, R.R.; Xu, Y. Computational Prediction of the Formation of Microporous Aluminophosphates with Desired Structural Features. *Microporous Mesoporous Mater.* **2010**, *129*, 251–255. [CrossRef]
30. Konstantin, I.; Galkin, K.I.; Krivodaeva, E.A.; Romashov, L.V.; Zalesskiy, S.S.; Kachala, V.V.; Burykina, J.V.; Ananikov, V.P. Critical Influence of 5-Hydroxymethylfurfural Aging and Decomposition on the Utility of Biomass Conversion in Organic Synthesis. *Angew. Chem. Int. Ed.* **2016**, *55*, 8338–8342.
31. Altomare, A.; Cuocci, C.; Giacovazzo, C.; Moliterni, A.; Rizzi, R.; Corriero, N.; Falcicchio, A. EXPO2013: A Kit of Tools for Phasing Crystal Structures from Powder Data. *J. Appl. Cryst.* **2013**, *46*, 1231–1235. [CrossRef]
32. Chowdhury, A.; Bhattacharjee, S.; Chatterjee, R.; Bhaumik, A. A New Nitrogen Rich Porous Organic Polymer for Ultra-High CO_2 Uptake and as An Excellent Organocatalyst for CO_2 Fixation Reactions. *J. CO2 Util.* **2022**, *65*, 102236. [CrossRef]
33. Shahangi, F.; Chermahini, A.N.; Saraji, M. Dehydration of fructose and glucose to 5-hydroxymethylfurfural over Al-KCC-1 silica. *J. Energy Chem.* **2018**, *27*, 769–780. [CrossRef]
34. Qiu, G.; Wang, X.; Huang, C.; Li, Y.; Chen, B. Niobium phosphotungstates: Excellent solid acid catalysts for the dehydration of fructose to 5-hydroxymethylfurfural under mild conditions. *RSC Adv.* **2018**, *8*, 32423–32433. [CrossRef] [PubMed]
35. Jiang, C.W.; Su, A.X.; Li, X.M. Preparation of Aluminosilicate Mesoporous Catalyst and its Application for Production 5-Hydroxymethyl Furfural Dehydration from Fructose. *Adv. Res. Mater.* **2011**, *396–398*, 1190–1193. [CrossRef]
36. Dutta, A.; Gupta, D.; Patra, A.K.; Saha, B.; Bhaumik, A. Synthesis of 5-Hydroxymethylfurural from Carbohydrates using Large-Pore Mesoporous Tin Phosphate. *ChemSusChem* **2014**, *7*, 925–933. [CrossRef]
37. Crisci, A.J.; Tucker, M.H.; Lee, M.Y.; Jang, S.G.; Dumesic, J.A.; Scott, S.L. Acid-Functionalized SBA-15-Type Silica Catalysts for Carbohydrate Dehydration. *ACS Catal.* **2011**, *1*, 719–728. [CrossRef]
38. Ghosh, A.; Chowdhury, B.; Bhaumik, A. Synthesis of Hollow Mesoporous Silica Nanospheroids with O/W Emulsion and Al(III) Incorporation and Its Catalytic Application. *Catalysts* **2023**, *13*, 354. [CrossRef]